

Integrin-mediated Membrane Blebbing Is Dependent on Sodium-Proton Exchanger 1 and Sodium-Calcium Exchanger 1 Activity^{*S}

Received for publication, March 29, 2011, and in revised form, December 23, 2011. Published, JBC Papers in Press, January 23, 2012, DOI 10.1074/jbc.M111.244962

Yung-Hsiang Yi^{‡S}, Yu-Sun Chang[‡], Chi-Hung Lin[¶], Tien-Shen Lew[¶], Chih-Yung Tang^{**}, Wei-Lien Tseng^{‡‡}, Ching-Ping Tseng^{‡‡}, and Szecheng J. Lo^{S¶1}

From the [‡]Molecular Medicine Research Center, ^SDepartment of Biomedical Sciences, and ^{‡‡}Department of Medical Biotechnology and Laboratory Science, Chang Gung University, Kwei-Shan, Tao-Yuan 333, Taiwan, R.O.C., the [¶]Institute of Microbiology and Immunology and ^{¶¶}Department of Physiology, National Yang-Ming University, Taipei 112, Taiwan, R.O.C., and the ^{**}Department of Physiology, National Taiwan University, Taipei 100, Taiwan, R.O.C.

Background: Integrin signaling and membrane blebbing modulate cell adhesion and migration, however, the link between them is unknown.

Results: NHE1 and NCX1 are located in the bleb membrane, where they modulate integrin-mediated membrane blebbing.

Conclusion: NHE1 and NCX1 functional coupling is important for bleb growth and retraction.

Significance: These data reveal novel functionality for NHE1 and NCX1 in both integrin signaling and membrane blebbing.

Integrin signaling and membrane blebbing modulate cell adhesion, spreading, and migration. However, the relationship between integrin signaling and membrane blebbing is unclear. Here, we show that an integrin-ligand interaction induces both membrane blebbing and changes in membrane permeability. Sodium-proton exchanger 1 (NHE1) and sodium-calcium exchanger 1 (NCX1) are membrane proteins located on the bleb membrane. Inhibition of NHE1 disrupts membrane blebbing and decreases changes in membrane permeability. However, inhibition of NCX1 enhances cell blebbing; cells become swollen because of NHE1 induced intracellular sodium accumulation. Our study found that NHE1 induced sodium influx is a driving force for membrane bleb growth, while sodium efflux (and calcium influx) induced by NCX1 in a reverse mode results in membrane bleb retraction. Together, these findings reveal a novel function for NHE1 and NCX1 in membrane blebbing and permeability, and establish a link between membrane blebbing and integrin signaling.

Animal cell plasma membranes undergo dynamic local expansion and retraction to form transient, small spherical blebs. Local disruption of the plasma membrane interaction with the actin submembrane cortex initiates bleb formation, followed by lipid incorporation into the bleb site (1–3). The blebs expand (membrane bleb growth) by transient increases in intracellular pressure accompanied by reassembly of F-actin in the bleb cortex by an unknown mechanism, which then acts as a track for sliding of myosin motors (membrane bleb retraction) (3). Membrane blebbing is associated with many cellular activities, such as cell adhesion, spreading, migra-

tion, virus entry, cytokinesis, and apoptosis (1–4). Although integrin receptors, which are heterodimers formed by combination of 18 α and 8 β subunits, and their extracellular matrix ligand proteins, either collagen, laminin, or fibronectin, also regulate many of these cellular activities (5, 6), it is unclear whether integrin-mediated signals are involved in membrane blebbing.

Based on ligand specificity and restricted expression in leukocytes, the 24 known integrins are divided into four subfamilies, arginine-glycine-aspartate (RGD)² motif receptors, collagen receptors, laminin receptors, and leukocyte-specific receptors (5, 6). Integrin $_{\alpha_{IIb}\beta_3}$ (the dominant integrin in blood platelets) is an RGD receptor that modulates platelet adhesion and spreading, critical for thrombosis (7–9). Previously, we demonstrated that activation of platelet and CHO $_{\alpha_{IIb}\beta_3}$ cells (recombinant CHO cells expressing the human integrin $_{\alpha_{IIb}\beta_3}$ protein) by fibrinogen and recombinant rhodostomin (RGD-containing protein from *Agkistrodon rhodostoma* snake venom), can induce cell adhesion, spreading, and intracellular calcium oscillation (10–14). We also reported that integrin $_{\alpha_{IIb}\beta_3}$ downstream signals induced an interaction of NHE1-integrin $_{\alpha_{IIb}\beta_3}$ -NCX1 on intracellular vesicles then targeting to the plasma membrane, leading to the formation of functional complexes in lipid raft microdomains (15, 16). NHE1 and NCX1 both appear in homodimeric forms and are functionally coupled; NHE1 drives sodium ion influx, which in turn activates NCX1 in a reverse mode to generate a calcium influx and modulate intracellular calcium oscillations (15, 17–20). It is not clear if integrin signaling generally triggers ion transport. In this study, we employed whole cell voltage-clamp techniques to

* This work was supported by grants from the Chang Gung Memorial Hospital, the Ministry of Education, and the National Science Council, R.O.C.

^S This article contains supplemental movies S1–S5.

¹ To whom correspondence should be addressed: Department of Biomedical Sciences, Chang Gung University, Tao-Yuan 333, Taiwan. Tel.: 886-3-2118800 ext. 3295; Fax: 886-3-2118392; E-mail: losj@mail.cgu.edu.tw.

² The abbreviations used are: RGD, arginine-glycine-aspartate; CHO $_{\alpha_{IIb}\beta_3}$, Chinese Hamster Ovary cells expressing human integrin $_{\alpha_{IIb}}$ and integrin $_{\beta_3}$; NHE1, sodium-proton exchanger 1; NCX1, sodium-calcium exchanger 1; EIPA, 5-(N-ethyl-N-isopropyl)-amiloride; DIC, differential interference contrast.

measure the ion flow when cells contacted with various substrates, including fibrinogen and rhodostomin. Additionally, we recorded cell membrane activity by time-lapse microscopy to observed membrane blebbing.

EXPERIMENTAL PROCEDURES

Cell Models, Preparation of Substrates, and Pharmacological Treatments—Chinese hamster ovary cells expressing human integrin $_{\alpha 11b}$ and integrin $_{\beta 3}$ (CHO $_{\alpha 11b\beta 3}$), and Chinese Hamster Ovary cells expressing human integrin $_{\alpha v}$ and integrin $_{\beta 3}$ (CHO $_{\alpha v\beta 3}$) cell lines were gifted by Dr. M. H. Ginsberg (The Scripps Research Institute, La Jolla, CA) and Dr. Y. Takata (University of California-Davis, School of Medicine). Purification of recombinant rhodostomin (both wild-type RGD and mutant RGE) and the isolation of human platelets from volunteers were performed as previously described (13). Human fibrinogen, fibronectin, poly-L-lysine, bovine serum albumin (BSA), *n*-methyl-D-glucamine (NMG), bepridil, and 5-(*N*-ethyl-*N*-isopropyl)-amiloride (EIPA) were purchased from Sigma. Sodium Green fluorescent dye was obtained from Molecular Probes, Inc. (Eugene, OR). Preparation of substrates (fibrinogen, fibronectin, recombinant rhodostomin, and poly-L-lysine) at 4×10^{-7} M concentration was carried out as previously described (12).

Whole Cell Voltage-Clamp Recording—For whole cell voltage-clamp recording, we used a commercially available amplifier and data acquisition software (Axopatch 200B, Axon Instruments, Union City, CA). For the preparation of cell suspensions, cells were harvested using a $1 \times$ trypsin solution, and dissociated using Dulbecco's modified Eagles' medium (supplemented with 10% fetal bovine serum) (Invitrogen). Cells were kept in suspension for 10 min in the presence or absence of EIPA (25 μ M) before use. Suspended cells were plated onto various substrates for 5 min prior to transfer to the recording chamber containing an extracellular electrolyte solution. Whole cell voltage-clamp recording was carried out in the chamber under a phase contrast microscope (DM IRE, Leica Microsystems, Wetzlar, Germany). Membranes were clamped at -40 mV and current changes continuously recorded for 10 min. The intracellular electrolyte solution was composed NaCl (140 mM), KCl (5 mM), MgCl $_2$ (2 mM), and HEPES (5 mM) at pH 7.35. The extracellular electrolyte solution was prepared as per the intracellular electrolyte solution, with the further addition of CaCl $_2$ (1 mM). For ion substitution experiments, sodium was replaced by an equal molar amount of *N*-methyl-D-glucamine.

Live Cell Imaging—Live cell and sodium images were recorded according to previously described methods with some modifications (15). Suspended cells were pretreated in the presence or absence of EIPA (25 μ M for CHO $_{\alpha 11b\beta 3}$ cell, 100 μ M for NIH3T3 cell) or bepridil (80 μ M) for 10 min, and then plated for 5 min, in preparation for phase contrast, differential interference contrast, and fluorescence time-lapse microscopy. Cells were observed under these various microscopic methods in a climate chamber, to maintain cell viability and activity. Images were recorded at 5-s intervals. For sodium imaging, suspended cells were labeled either with 2 μ M Sodium Green dye at 37 $^{\circ}$ C for 10 min in the presence or absence of EIPA (100 μ M)

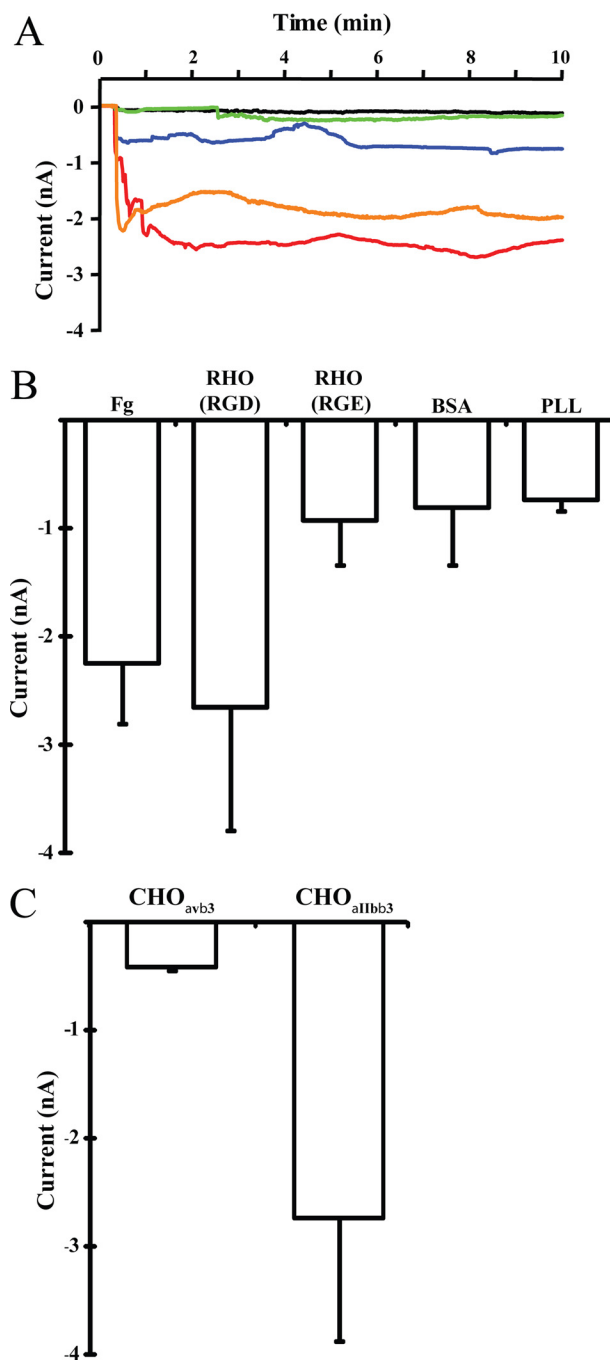
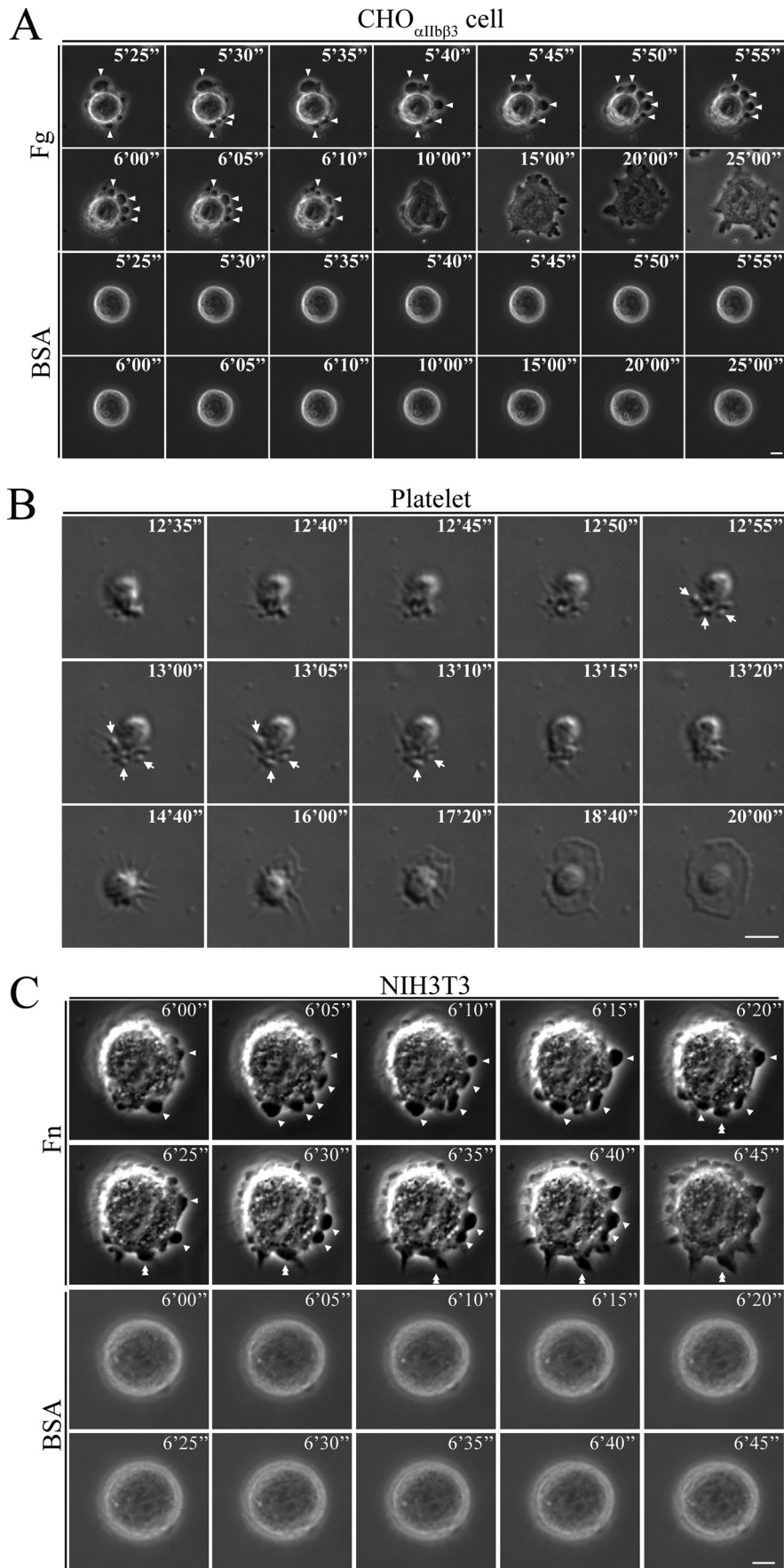


FIGURE 1. Detection of integrin $_{\alpha 11b\beta 3}$ -mediated membrane permeability changes by the whole cell voltage-clamp technique. A, CHO $_{\alpha 11b\beta 3}$ cells were attached onto different substrates and membrane permeability changes monitored by whole cell voltage-clamp recording. The current change of cells attached onto various substrates are shown as different color traces: CHO $_{\alpha 11b\beta 3}$ cell onto fibrinogen (Fg), orange trace; rhodostomin (RGD) (RHO (RGD), wild type), red trace; rhodostomin (RGE) (RHO (RGE), mutant), blue trace; BSA, green trace; poly-L-lysine (PLL), black trace. B, summary of membrane permeability changes data from three independent experiments as shown in panel A. Note that integrin $_{\alpha 11b\beta 3}$ specific substrates fibrinogen and rhodostomin (RGD) induce membrane permeability changes. The numbers (*n*) of cells recorded for each substrate were: fibrinogen, *n* = 6; rhodostomin (RGD), *n* = 12; rhodostomin (RGE), *n* = 4; BSA, *n* = 13; poly-L-lysine, *n* = 3. C, CHO $_{\alpha v\beta 3}$ and CHO $_{\alpha 11b\beta 3}$ cells were attached onto the rhodostomin (RGD) substrate and the membrane permeability monitored using whole cell voltage-clamp recording. Note that rhodostomin (RGD) induced membrane permeability changes were observed in CHO cells expressing integrin $_{\alpha 11b\beta 3}$ but not integrin $_{\alpha v\beta 3}$. The numbers (*n*) of cells recorded for each cell line were: CHO $_{\alpha v\beta 3}$, *n* = 4; CHO $_{\alpha 11b\beta 3}$, *n* = 7. Error bars indicate S.E.

Role of NHE1 and NCX1 in Membrane Blebbing



before cell plating. Fluorescence signals were recorded (532 nm) at 20-s intervals, and then converted into pseudo-color using the MetaMorph software version 6.1 (Universal Imaging, Downingtown, PA).

Immunofluorescence Staining—Suspended cells were plated for 10 min and subjected to immunofluorescence staining using previously described methods (15). Antibody probes and concentrations were used as follows: integrin $_{\alpha\text{IIb}\beta\text{3}}$ antibodies (1:100 dilution) (Chemicon, Temecula, CA), NHE-1 (1:100 dilution), NCX-1 (1:100 dilution), and CD45 (1:100 dilution) (Santa Cruz Biotechnology, Inc., Santa Cruz, CA). Fluorochrome-conjugated secondary antibodies (1:200 dilution) were obtained from Jackson Laboratories (West Grove, PA). All stained samples were observed under a BD CARV IITM confocal microscope (BD Bioscience, San Jose, CA).

RESULTS

Integrin $_{\alpha\text{IIb}\beta\text{3}}$ -Ligand Interaction Induces Changes in Membrane Permeability—We used whole cell voltage-clamp recording to measure ionic flow across the plasma membrane, to investigate if plating CHO $_{\alpha\text{IIb}\beta\text{3}}$ cells onto fibrinogen or rhodostomin (RGD wild type) substrates induced changes in ion current (Fig. 1A). From representative data, there were changes in ion current of approximately -1.5 to -2.5 nA during the first 10 min, as cells attached onto fibrinogen or rhodostomin (RGD) substrates (orange and red trace). Fig. 1B summarizes quantitative data from 6 and 12 individual cells attached onto fibrinogen and rhodostomin (RGD) substrates respectively. Plating CHO $_{\alpha\text{IIb}\beta\text{3}}$ cells onto rhodostomin (RGE mutant, a glutamic acid-substituted rhodostomin), BSA, or poly-L-lysine (PLL)-coated substrates (Fig. 1, A and B) did not produce any change in membrane permeability. Nor did we observe any change in membrane permeability when parental CHO cells (data not shown) and CHO cells expressing integrin $_{\alpha\text{v}\beta\text{3}}$ were plated onto the rhodostomin (RGD)-coated substrate (Fig. 1C). The observed change in membrane permeability was specific to integrin $_{\alpha\text{IIb}\beta\text{3}}$ -ligand interactions. Thus, activation of integrin $_{\alpha\text{IIb}\beta\text{3}}$ induces changes in cell membrane permeability.

Integrin-Ligand Interaction Induces Cell Membrane Blebbing at an Early Stage of Cell Spreading—During the execution of the experiments on membrane permeability, we monitored membrane blebbing by time-lapse phase-contrast microscopy. Attaching CHO $_{\alpha\text{IIb}\beta\text{3}}$ cells onto the fibrinogen-coated substrate produced blebbing before cell spreading occurred (arrowheads in upper panels of Fig. 2A and in supplemental movie S1). Few CHO $_{\alpha\text{IIb}\beta\text{3}}$ cells attached to the BSA-coated substrate control did not produce noticeable blebbing (Fig. 2A, lower panels). We tested human platelet cells, abundant in integrin $_{\alpha\text{IIb}\beta\text{3}}$, to determine whether integrin-induced mem-

brane blebbing occurs for other cell types. We observed membrane blebbing from platelets when seeded onto fibrinogen-coated substrate before spreading occurred (arrows in Fig. 2B and supplemental movie S2). We observed similar results after plating NIH3T3 cells, a mouse fibroblast cell containing two members of the RGD receptor (integrin $_{\alpha\text{v}\beta\text{3}}$ and integrin $_{\alpha\text{5}\beta\text{1}}$) (21), onto fibronectin-coated substrate (arrowheads in upper panels of Fig. 2C and supplemental movie S3). Occasionally, filopodium elongation occurred at the membrane blebbing site of NIH3T3 cell (double arrowheads in upper panels of Fig. 2C). By contrast, most NIH3T3 cells attached onto BSA-coated plates did not produce noticeable blebbing (Fig. 2C and supplemental movie S4). Taken together, these data demonstrate that for various cell types, integrin-ligand interactions induce membrane blebbing prior to cell spreading.

NHE1 Localizes to the Bleb Membrane and Modulates Membrane Bleb Growth and Membrane Permeability—Previous work established that downstream signals of integrin $_{\alpha\text{IIb}\beta\text{3}}$ can target NHE1 and NCX1 to the plasma membrane (15), and that NHE1- and NCX1-associated proteins are present in membrane blebs (2, 3, 22–25). We were interested to find out if the membrane blebs contain the two cation exchangers and if so, to determine if the exchangers are involved in either inducing membrane blebbing, or in the observed permeability changes, or both. After attaching CHO $_{\alpha\text{IIb}\beta\text{3}}$ cells onto the fibrinogen substrate, immunofluorescent antibody staining revealed the presence of NHE1 (Fig. 3A, first row) but not CD45 (a control membrane protein; Fig. 3A, second row) in the bleb membrane. However, the few CHO $_{\alpha\text{IIb}\beta\text{3}}$ cells attached onto BSA-coated substrate did not show noticeable bleb formation (Fig. 3A, third row). We identified NHE1 in the bleb membranes of 83% of cells, while no CD45 was detected (Fig. 3B). No membrane blebs appeared from CHO $_{\alpha\text{IIb}\beta\text{3}}$ or NIH3T3 cells attached to fibrinogen or fibronectin substrates after pretreatment with NHE1 inhibitor (EIPA) (Fig. 3, C and D). Moreover, EIPA also blocked changes in membrane permeability (Fig. 3, E and F). These data suggest that NHE1, which can pump sodium ions into cells, is required for integrin-mediated cell membrane blebbing and membrane permeability changes.

NCX1 Localizes to the Bleb Membrane and Compensates the NHE1-mediated Sodium Influx in a Reverse Mode—NHE1 and NCX1 are functionally coupled (15), and so we investigated the role of NCX1 in membrane blebbing by treating CHO $_{\alpha\text{IIb}\beta\text{3}}$ cells with an NCX1 inhibitor (bepridil). Immunofluorescent antibody staining revealed that NCX1 (Fig. 4A, first row), but not CD45 (Fig. 4A, second row), was present in the bleb membranes of untreated CHO $_{\alpha\text{IIb}\beta\text{3}}$ cells attached onto fibrinogen substrate. There was no noticeable bleb formation from cells

FIGURE 2. Membrane blebbing for cells attached onto various substrates. A, CHO $_{\alpha\text{IIb}\beta\text{3}}$ cells attached onto fibrinogen or BSA control substrates. A selected time-lapse phase-contrast microscopy image sequence is shown. Note that the fibrinogen substrate (upper panels, arrowheads), not the BSA substrate (lower panels), induced cell membrane blebbing before the cell fully spread. B, platelet cells attached onto fibrinogen substrate. Time-lapse differential interference-contrast microscopy imaging was used to monitor membrane blebbing and spreading. The fibrinogen substrate induced cell membrane blebbing (arrows) before the platelet cell was fully spread. C, time-lapse phase-contrast microscopy images of NIH3T3 cells attached onto fibronectin and control BSA substrates. Note that cell membrane blebbing occurred before the cells were fully spread when induced by the fibronectin substrate (upper panels, arrowheads), but not by BSA substrate (lower panels). Single filopodium elongation occurring at the blebbing site is indicated by the double arrowheads. Numbers on panels A–C indicate time in min. Scale bar represents 5 μm .

Role of NHE1 and NCX1 in Membrane Blebbing

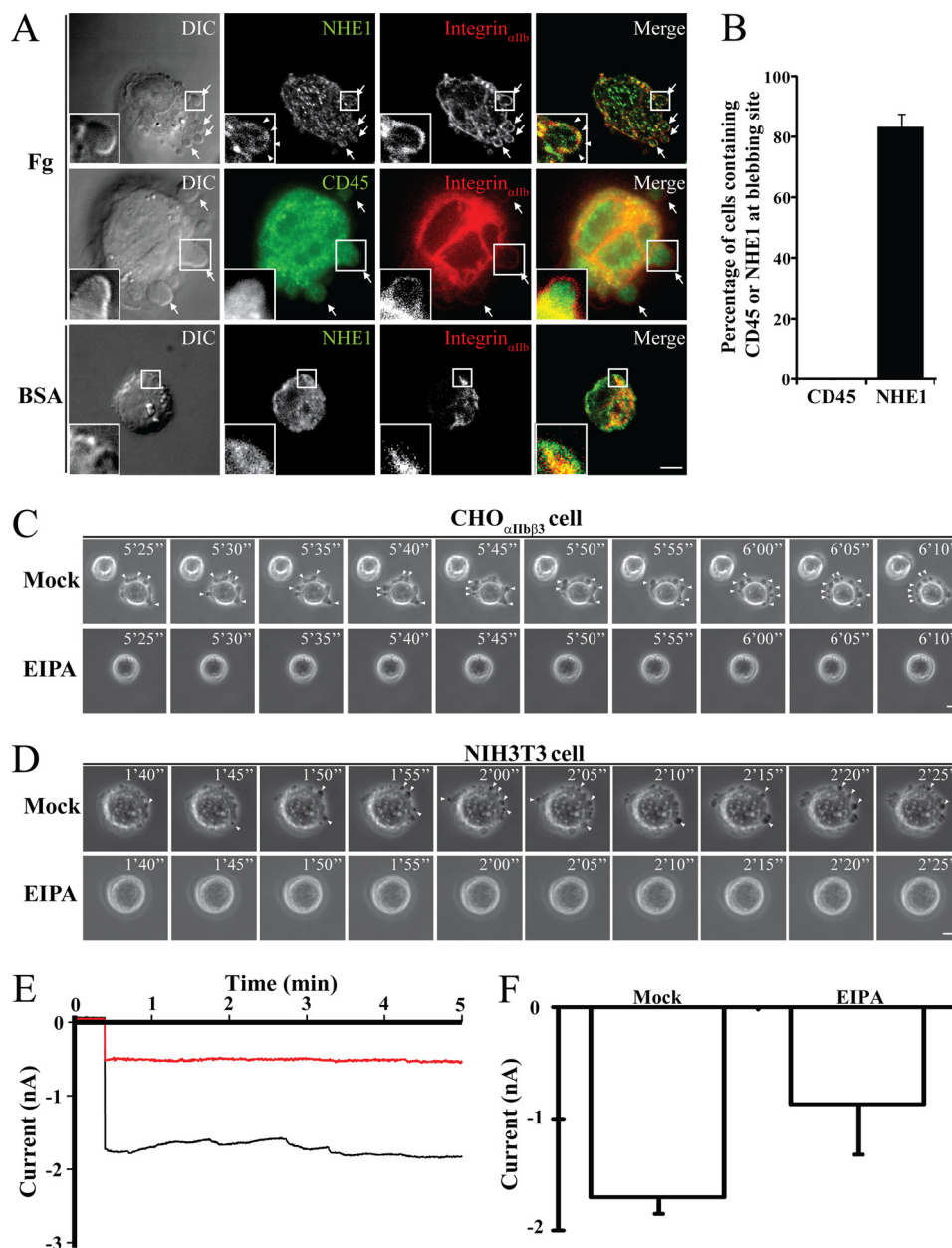


FIGURE 3. Analyses of NHE1 distribution in bleb membranes and the role of NHE1 in membrane blebbing and permeability changes. *A*, CHO_{α11bβ3} cells, plated onto fibrinogen or BSA substrates, were stained with fluorescently-tagged immunoglobulins to highlight NHE1, integrin_{α11b}, and CD45 distributions. Cell images were recorded under a DIC microscope (left panel) and fluorescence microscope (three right panels). Membrane blebs were observed when CHO_{α11bβ3} cells were plated onto fibrinogen substrate (first and second rows, arrows) but not on BSA substrate (third row). The merged images show co-localization of integrin_{α11b} and NHE1 (right panel). Note that NHE1 (insets of the first row, arrowheads), but not CD45 (insets of the second row), is located in the bleb membrane when plated onto fibrinogen substrate. The insets in each panel are enlarged from the portion of the cell indicated by a square box. *B*, percentage of cells with bleb-associated NHE1 ($n = 51$ cells) or CD45 ($n = 49$ cells) from three independent experiments such as those in *A* are shown. Note that NHE1, but not CD45, was present in the bleb membrane when CHO_{α11bβ3} cells were seeded onto the fibrinogen substrate. *C*, CHO_{α11bβ3} or (*D*) NIH3T3 cells pretreated with or without NHE1 inhibitor (EIPA) were seeded onto fibrinogen or fibronectin substrates. Time-lapse phase-contrast microscopy images were taken at 5-s intervals. The scale bars in panels *A*, *C*, and *D* represent 5 μm . Note that bleb growth was induced by fibrinogen or fibronectin substrates (upper panels, arrowheads) but was inhibited by EIPA pretreatment (lower panels). Numbers on panels *C* and *D* indicate time in min. *E*, membrane permeability changes of CHO_{α11bβ3} cells attached onto a rhodostomin (RGD) substrate in the presence (red trace) or in the absence (black trace) of EIPA. Membrane permeability changes were measured by whole cell voltage-clamp recording. *F*, summary of membrane permeability change data from three independent experiments as shown in panel *E*. The numbers (n) of cells recorded for each treatment were: mock, $n = 6$; EIPA, $n = 5$. Error bars indicate S.E.

plated onto the BSA substrate (Fig. 4*A*, third row). Analysis of three independent experiments showed the presence of NCX1 on bleb membranes in 26% of cells, while no CD45 was detected (Fig. 4*B*). Moreover, we found that CHO_{α11bβ3} cells pretreated with bepridil produced enlarged membrane blebs, and the cells themselves became swollen (double arrowheads, Fig. 4*C*). Pre-

viously, we reported that cell swelling accompanies intracellular sodium accumulation in bepridil-pretreated CHO_{α11bβ3} cells attached onto fibrinogen substrate (15). Sodium accumulation also occurred in the membrane blebs of NIH3T3 cells when attached to fibronectin substrate (arrows in Fig. 4*D* and supplemental movie S5). Few EIPA-pretreated NIH3T3 cells

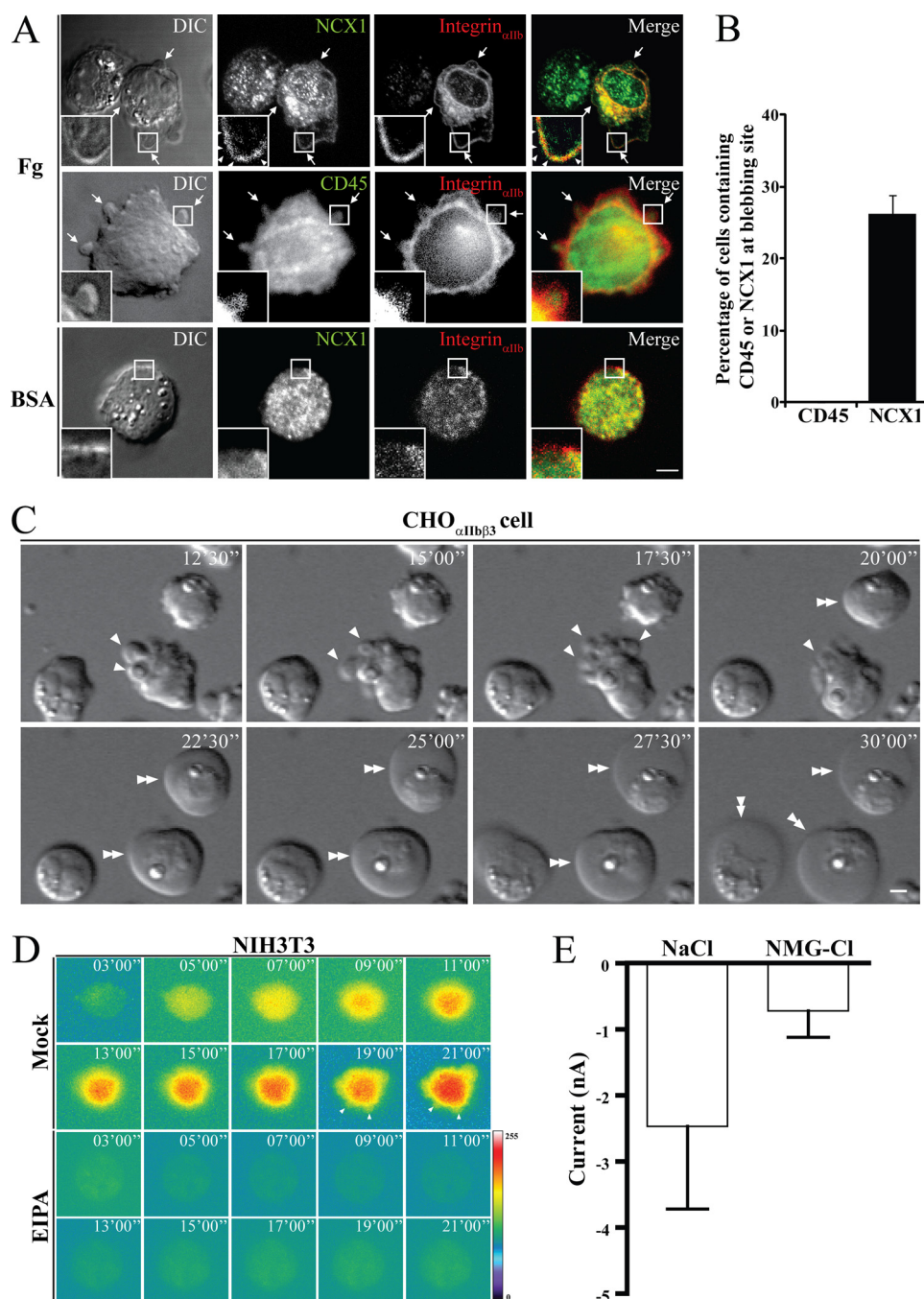


FIGURE 4. Analyses of NCX1 distribution in bleb membranes and the role of NCX1 in membrane blebbing and permeability changes. *A*, immunostaining of CHO $_{\alpha IIb\beta 3}$ cells plated onto fibrinogen or BSA substrates to observe NCX1, integrin $_{\alpha IIb\beta 3}$, and CD45 distribution. Cell images were obtained using DIC and fluorescence microscopy. Note that NCX1 (first row insets, arrowheads), but not CD45 (second row insets), is located in the bleb membrane when cells were attached to the fibrinogen substrate. *B*, percentage of cells with bleb-associated NCX1 ($n = 53$ cells) or CD45 ($n = 50$ cells) from three independent experiments such as those in *A* are shown. *C*, time-lapse differential interference contrast microscopy imaging of CHO $_{\alpha IIb\beta 3}$ cells attached onto a rhodostomin (RGD) substrate in the presence of bepridil. Note that bleb enlargement occurred (single arrows) and cells became swollen (double arrowheads) when the cells were pretreated with bepridil, and attached onto the rhodostomin (RGD) substrate. *D*, sodium ion distribution in NIH3T3 cells attached to fibronectin substrate in the presence, or absence, of EIPA. A selected time-lapse fluorescence image sequence is shown. Arrowheads indicate the membrane blebs. *E*, quantitative data of membrane permeability changes when CHO $_{\alpha IIb\beta 3}$ cells attached onto rhodostomin (RGD) substrate in various pipette solutions as indicated. Note that replacing intracellular sodium ion with NMG-Cl significantly reduced the magnitude of membrane permeability changes. The numbers (n) of cells recorded for each condition were: NaCl, $n = 7$; NMG-Cl, $n = 4$. Numbers on panels *C* and *D* indicate time in min. Scale bar represents 5 μm .

attached onto fibronectin substrate, and they did not show any noticeable increases in intracellular sodium (Fig. 4*D*). To investigate the role of NCX1 in changes of membrane permeability, *N*-methyl-D-glucamine (the inhibitor of sodium transport) was applied to replace intracellular sodium. Whole-cell voltage-

clamp recording revealed that *N*-methyl-D-glucamine replacement inhibited sodium efflux and reduced membrane permeability to 0.8 nA (Fig. 4*E*). These data suggest that NCX1, which can operate reversibly and generate sodium efflux, counteracts NHE1-mediated sodium influx in these cells.

Role of NHE1 and NCX1 in Membrane Blebbing

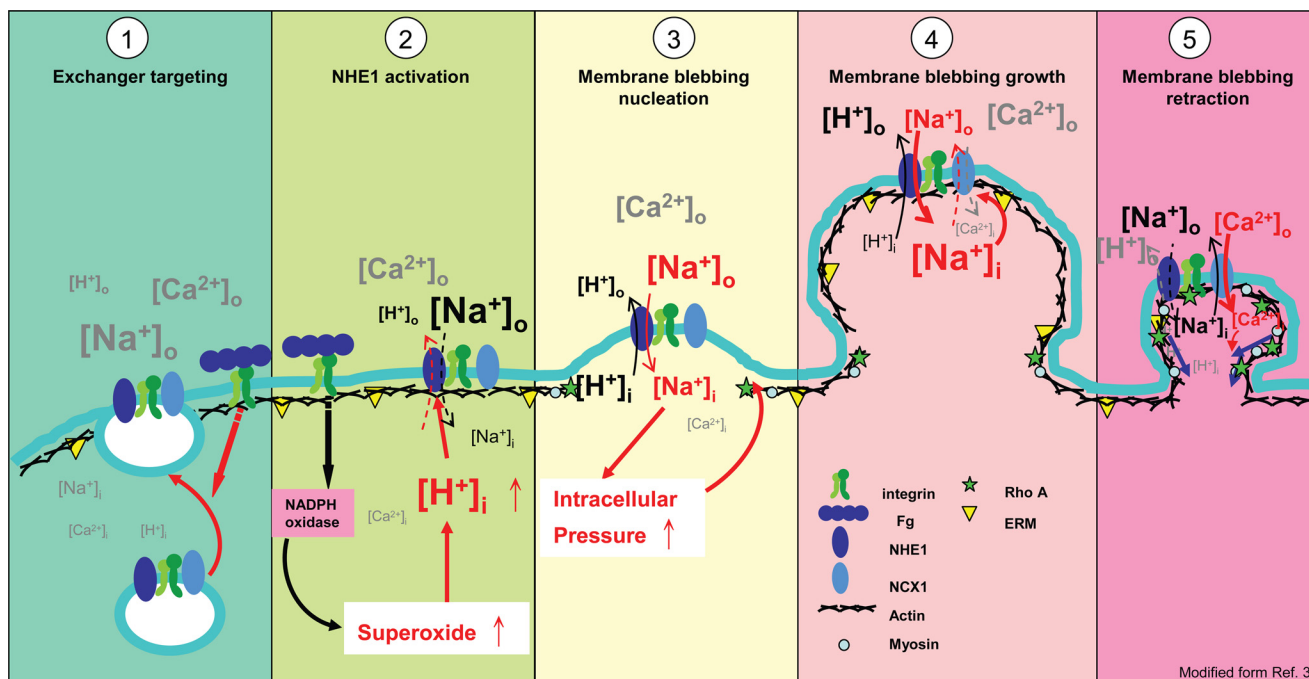


FIGURE 5. Model hypothesis modified from Ref. 3 that integrin-mediated membrane blebbing is dependent on the activities of NHE1 and NCX1 (panel 1). Integrin-ligand interactions induce targeting of NHE1 and NCX1-containing vesicles onto the plasma membrane (panel 2). After cell attachment onto a substrate, NADPH oxidase is activated through integrin signals and increases the levels of superoxide and lowers pH (cytosolic acidification), which in turn activates NHE1 to cause proton efflux (cytosolic alkalization) and coupled sodium influx (panel 3). The sodium influx further increases intracellular pressure, a driving force that causes membrane bleb nucleation and growth (panel 4). Increased intracellular sodium concentration activates NCX1 in a reverse mode to cause the efflux of intracellular sodium and calcium influx (panel 5). The local increase in intracellular calcium driven by NCX1 induces myosin-mediated contraction and membrane bleb retraction. The figure symbols are indicated, and the various ion symbol sizes represent the relative concentrations of ions in intracellular (i) or extracellular (o) compartments.

DISCUSSION

Membrane blebbing is associated with many cellular activities, such as cell spreading, cell migration, virus entry, cytokinesis, and apoptosis. Nevertheless, little is known about the detailed mechanisms (1–4). Our observations show that integrin $_{\alpha_{11b}\beta_3}$ signals, which mediate cell spreading, induce membrane blebbing in CHO $_{\alpha_{11b}\beta_3}$ cells (Fig. 2A). Membrane blebbing was also observed on human platelet cells, when they adhere onto a fibrinogen substrate, and before they are fully spreading (Fig. 2B), indicating that signals downstream of integrin $_{\alpha_{11b}\beta_3}$ -ligand binding can induce membrane blebbing. Membrane blebbing also occurred when NIH3T3 cells adhere onto fibronectin substrate (Fig. 2C), and together with results from CHO $_{\alpha_{11b}\beta_3}$ cells and platelets (Fig. 2, A and B), these data suggest that integrin-ligand interactions induce cell adhesion to the solid substrate, and that membrane blebbing is a common phenomenon that occurs in the early stages of cell spreading (4).

Cell spreading and migration accompany NHE1 modulated changes in cell volume (22–24, 26, 27). However, it is not clear whether NHE1 is required for changes in integrin $_{\alpha_{11b}\beta_3}$ -mediated permeability or membrane blebbing during cell spreading. Our study links the two cation exchangers, NHE1 and NCX1, to integrin $_{\alpha_{11b}\beta_3}$ -mediated changes in membrane permeability and blebbing. As shown in Figs. 3B and 4B, there are a greater percentage of cells with NHE1 in the bleb membrane (85%) than there are cells with NCX1 in the bleb membrane (26%). This may suggest that the bleb membrane contains a greater amount of NHE1 protein than it does NCX1. In many animal

cells, NHE1 operates in parallel with a $\text{Cl}^-/\text{HCO}_3^-$ anion exchanger, which allows cells to take up sodium and chloride ions (26). This uptake can drive the influx of water by osmosis, resulting in increases in cellular volume and intracellular (osmotic) pressure, causing cell blebbing and swelling (26).

Many proteins associated with actin, including ERM protein, Rho A, ROCK, and ankyrin interact with NHE1 or NCX1 (22–25) and are present in membrane blebs (2, 3). Additionally, sodium and calcium are enriched in membrane blebs of inner hair cell (28), zebrafish primordial germ cells (29), and NIH3T3 cells (Fig. 4C). We modified the membrane blebbing model proposed by Fackler and Grosse (3), hypothesizing that NHE1 and NCX1 coupling plays a role in membrane blebbing, driving the influx of calcium, and subsequent actin-filament formation and myosin sliding to control the dynamic changes of membranes (Fig. 5). When integrins are activated by binding to their protein substrates, vesicular NHE1 and NCX1 are targeted to the plasma membrane (15) (Fig. 5, panel 1).

Previous studies of human neutrophil adherence and spreading on fibrinogen-coated slides revealed these processes to be β_2 -integrin mediated with concomitant activation of NADPH oxidase (30). Activation of NADPH oxidase increases superoxide production and causes cytosolic acidification, which in turn activates NHE1 and rapid alkalization of the cytoplasm. Thus, it is probable that downstream integrin signaling, followed by elevation of superoxide and proton concentrations by NADPH oxidase, activates NHE1, causing subsequent cytosolic alkalization and sodium ion influx (Fig. 5, panels 2 and 3). Sodium ion influx can increase cellular volume and intracellular pressure

(22), an initial driving force that triggers membrane bleb growth by forming a membrane-blebbing nucleation site (15) (Figs. 4C and 5, panel 3). As sodium influx continues, the membrane bleb grows, which triggers NCX1 to operate reversibly in bleb membrane and so decreases intracellular pressure by refluxing sodium ions out from the cells and influxing calcium ions into cells (15, 31, 32) (Figs. 4 and 5, panel 4). As demonstrated by the zebrafish primordial germ cell study described above, calcium ion accumulates in the membrane bleb region inducing myosin-mediated contraction, accompanied by activation of actin-associated proteins located underneath the membrane bleb, so causing membrane bleb retraction (Fig. 5, panel 5) (3, 29).

Previous studies on NHE1 and NCX1 focused on their roles in maintaining ion homeostasis in cardiac myocytes (33), and some studies demonstrated that NHE1 is involved in the cell migration (18–20). Our results demonstrate that both NHE1 and NCX1 play roles in maintaining membrane blebbing, which is involved in cell migration (1–4). There are forms of integrin-dependent metastatic cancer (34), and we speculate that up-regulation of NHE1 and NCX1 might occur in these cells. These two cation exchangers could provide new useful biomarkers of metastatic cancers, a hypothesis we are currently testing.

Acknowledgments—We thank Scott C. Schuyler (CGU), Simon Silver (CGU visiting professor), and Tung-Tien Sun (New York University) for reviewing the manuscript. We thank two anonymous reviews for their suggestions to the manuscript and NOVA Medical Documentation for proofreading service. We thank Dr. Tsung-Yu Chen (National Yang-Ming University) for providing electrophysiology equipment. Chang Gung University, the Biophotonics Interdisciplinary Research Center, and the Genome Research Center of National Yang-Ming University provided and supported microscopy services.

REFERENCES

- Charras, G. T. (2008) A short history of blebbing. *J. Microsc.* **231**, 466–478
- Charras, G., and Paluch, E. (2008) Blebs lead the way: how to migrate without lamellipodia. *Nat. Rev. Mol. Cell Biol.* **9**, 730–736
- Fackler, O. T., and Grosse, R. (2008) Cell motility through plasma membrane blebbing. *J. Cell Biol.* **181**, 879–884
- Norman, L., Sengupta, K., and Aranda-Espinoza, H. (2011) Blebbing dynamics during endothelial cell spreading. *Eur. J. Cell Biol.* **90**, 37–48
- Hynes, R. O. (2002) Integrins: bidirectional, allosteric signaling machines. *Cell* **110**, 673–687
- Barczyk, M., Carracedo, S., and Gullberg, D. (2010) Integrins. *Cell Tissue Res.* **339**, 269–280
- Varga-Szabo, D., Pleines, I., and Nieswandt, B. (2008) Cell adhesion mechanisms in platelets. *Arterioscler. Thromb. Vasc. Biol.* **28**, 403–412
- Salsmann, A., Schaffner-Reckinger, E., and Kieffer, N. (2006) RGD, the Rho'd to cell spreading. *Eur. J. Cell Biol.* **85**, 249–254
- Goncalves, I., Hughan, S. C., Schoenwaelder, S. M., Yap, C. L., Yuan, Y., and Jackson, S. P. (2003) Integrin α IIb β 3-dependent calcium signals regulate platelet-fibrinogen interactions under flow. Involvement of phospholipase C γ 2. *J. Biol. Chem.* **278**, 34812–34822
- Chang, H. H., Tsai, W. J., and Lo, S. J. (1997) Glutathione S-transferase-rhodostomin fusion protein inhibits platelet aggregation and induces platelet shape change. *Toxicon* **35**, 195–204
- Chang, H. H., Chang, C. P., Chang, J. C., Dung, S. Z., and Lo, S. J. (1997) Application of recombinant rhodostomin in studying cell adhesion. *J. Biomed. Sci.* **4**, 235–243
- Chang, H. H., Lin, C. H., and Lo, S. J. (1999) Recombinant rhodostomin substrates induce transformation and active calcium oscillation in human platelets. *Exp. Cell Res.* **250**, 387–400
- Chang, C. P., Chang, J. C., Chang, H. H., Tsai, W. J., and Lo, S. J. (2001) Positional importance of Pro53 adjacent to the Arg49-Gly50-Asp51 sequence of rhodostomin in binding to integrin α IIb β 3. *Biochem. J.* **357**, 57–64
- Hsieh, C. F., Chang, B. J., Pai, C. H., Chen, H. Y., Tsai, J. W., Yi, Y. H., Chiang, Y. T., Wang, D. W., Chi, S., Hsu, L., and Lin, C. H. (2006) Stepped changes of monovalent ligand-binding force during ligand-induced clustering of integrin α IIb β 3. *J. Biol. Chem.* **281**, 25466–25474
- Yi, Y. H., Ho, P. Y., Chen, T. W., Lin, W. J., Gukassyan, V., Tsai, T. H., Wang, D. W., Lew, T. S., Tang, C. Y., Lo, S. J., Chen, T. Y., Kao, F. J., and Lin, C. H. (2009) Membrane targeting and coupling of NHE1-integrin α IIb β 3-NCX1 by lipid rafts following integrin-ligand interactions trigger Ca^{2+} oscillations. *J. Biol. Chem.* **284**, 3855–3864
- Roberts, D. E., McNicol, A., and Bose, R. (2004) Mechanism of collagen activation in human platelets. *J. Biol. Chem.* **279**, 19421–19430
- Fafournoux, P., Noël, J., and Pouyssegur, J. (1994) Evidence that Na^+/H^+ exchanger isoforms NHE1 and NHE3 exist as stable dimers in membranes with a high degree of specificity for homodimers. *J. Biol. Chem.* **269**, 2589–2596
- Hisamitsu, T., Ben Ammar, Y., Nakamura, T. Y., and Wakabayashi, S. (2006) Dimerization is crucial for the function of the Na^+/H^+ exchanger NHE1. *Biochemistry* **45**, 13346–13355
- Fuster, D., Moe, O. W., and Hilgemann, D. W. (2008) Steady-state function of the ubiquitous mammalian Na/H exchanger (NHE1) in relation to dimer coupling models with 2Na/2H stoichiometry. *J. Gen. Physiol.* **132**, 465–480
- John, S. A., Ribalet, B., Weiss, J. N., Philipson, K. D., and Ottolia, M. (2011) Ca^{2+} -dependent structural rearrangements within $\text{Na}^+/\text{Ca}^{2+}$ exchanger dimers. *Proc. Natl. Acad. Sci. U.S.A.* **108**, 1699–1704
- Woods, D., Cherwinski, H., Venetsanakos, E., Bhat, A., Gysin, S., Humbert, M., Bray, P. F., Saylor, V. L., and McMahan, M. (2001) Induction of β 3-integrin gene expression by sustained activation of the Ras-regulated Raf-MEK-extracellular signal-regulated kinase signaling pathway. *Mol. Cell Biol.* **21**, 3192–3205
- Baumgartner, M., Patel, H., and Barber, D. L. (2004) Na^+/H^+ exchanger NHE1 as plasma membrane scaffold in the assembly of signaling complexes. *Am. J. Physiol. Cell Physiol.* **287**, C844–850
- Slepko, E. R., Rainey, J. K., Sykes, B. D., and Fliegel, L. (2007) Structural and functional analysis of the Na^+/H^+ exchanger. *Biochem. J.* **401**, 623–633
- Tominaga, T., and Barber, D. L. (1998) Na-H exchange acts downstream of RhoA to regulate integrin-induced cell adhesion and spreading. *Mol. Biol. Cell* **9**, 2287–2303
- Schulze, D. H., Muqhal, M., Lederer, W. J., and Ruknudin, A. M. (2003) Sodium/calcium exchanger (NCX1) macromolecular complex. *J. Biol. Chem.* **278**, 28849–28855
- Ritter, M., Fuerst, J., Wöll, E., Chwatal, S., Gschwenter, M., Lang, F., Deetjen, P., and Paulmichl, M. (2001) Na^+/H^+ exchangers: linking osmotic disequilibrium to modified cell function. *Cell Physiol. Biochem.* **11**, 1–18
- Stock, C., Cardone, R. A., Busco, G., Krähling, H., Schwab, A., and Reshkin, S. J. (2008) Protons extruded by NHE1: digestive or glue? *Eur. J. Cell Biol.* **87**, 591–599
- Shi, X., Gillespie, P. G., and Nuttall, A. L. (2005) Na^+ influx triggers bleb formation on inner hair cells. *Am. J. Physiol. Cell Physiol.* **288**, C1332–C1341
- Blaser, H., Reichman-Fried, M., Castanon, I., Dumstrei, K., Marlow, F. L., Kawakami, K., Solnica-Krezel, L., Heisenberg, C. P., and Raz, E. (2006) Migration of zebrafish primordial germ cells: a role for myosin contraction and cytoplasmic flow. *Dev. Cell* **11**, 613–627
- Demaurex, N., Downey, G. P., Waddell, T. K., and Grinstein, S. (1996) Intracellular pH regulation during spreading of human neutrophils. *J. Cell Biol.* **133**, 1391–1402

Role of NHE1 and NCX1 in Membrane Blebbing

31. Lytton, J. (2007) Na⁺/Ca²⁺ exchangers: three mammalian gene families control Ca²⁺ transport. *Biochem. J.* **406**, 365–382
32. Wu, M. P., Kao, L. S., Liao, H. T., and Pan, C. Y. (2008) Reverse mode Na⁺/Ca²⁺ exchangers trigger the release of Ca²⁺ from intracellular Ca²⁺ stores in cultured rat embryonic cortical neurons. *Brain Res.* **1201**, 41–51
33. Hilgemann, D. W., Yaradanakul, A., Wang, Y., and Fuster, D. (2006) Molecular control of cardiac sodium homeostasis in health and disease. *J. Cardiovasc. Electrophysiol.* **17**, Suppl. 1, S47–S56
34. Desgrosellier, J. S., and Cheresh, D. A. (2010) Integrins in cancer: biological implications and therapeutic opportunities. *Nat. Rev. Cancer* **10**, 9–22